J Mater Sci (2007) 42:477–482
DOI 10.1007/s10853-006-1069-5

Synthesis of ZnO nanosheets by room-temperature decomposition of a layered precursor synthesized by microwave heating

Zhen-Hua Liang · Ying-Jie Zhu · Guo-Feng Cheng · Yue-Hong Huang

Received: 4 August 2005 / Accepted: 18 January 2006 / Published online: 31 October 2006

Abstract ZnO nanosheets with the wurtzite structure have been successfully synthesized via a microwave-assisted solution method. The thicknesses of ZnO nanosheets are in the range of 5–10 nm and lateral sizes up to 1 μm. The surfaces of ZnO nanosheets are $\pm(1\bar{2}10)$ planes of wurtzite structure. The as-prepared products were characterized by X-ray diffraction (XRD), transmission electron microscopy (TEM), high-resolution transmission electron microscopy (HRTEM). The optical and thermal properties were investigated with UV–Visible absorption spectra, thermogravimetric analysis (TG) and differential scanning calorimetric analysis (DSC).

Introduction

In recent years, many efforts in the field of nanomaterials have been focused on fabricating one-dimensional nanowires, nanorods and nanotubes [1]. Two-dimensional nanosheets can be regarded as a new class of nanostructured materials due to their high anisotropy and nanometer-scale thickness, possessing interesting properties [2–4]. Nanosheets are considered as ideal systems for investigating dimensionally confined transport phenomena and regarded as the ideal base to build functional devices on them. However, only a few kinds of metal oxide nanosheets have been reported up to now. For example, nanosheets of titania [3], manganese dioxide [5], $KCa_2Nb_3O_{10}$ [6] and $K_4Nb_6O_{17}$ [7] were synthesized by delamination of the layered precursor. Ga_2O_3 nanosheets and nanoribbons were synthesized by evaporating GaN at high temperatures in the presence of oxygen [8].

ZnO, a semiconductor with a direct band gap of 3.37 eV, has attracted increasing attention in recent years because of its excellent physical properties and thus many applications. ZnO has applications in gas sensors [9], catalysts [10], solar cells [11], transparent conductive oxides [12], optoelectronic devices [13] and piezoelectric devices [14]. Additionally, nanolasers based on highly oriented ZnO nanowires were reported [15]. Nanowire transistors were also reported recently [16]. To date, most synthetic efforts on ZnO have been directed towards its nnaowires, nanorods [17, 18], and nanoribbons [19]. Compared with one-dimensional ZnO nanostructures, relatively few studies on two-dimensional ZnO nanostructures have been reported [4, 20–23]. The reported methods were usually carried out at high temperatures.

Since the first reports of microwave-assisted liquid phase organic synthesis in 1986 [24, 25], the application of microwave heating in synthetic chemistry has been a fast growing area of research. Compared with conventional heating methods, microwave heating has been accepted as a promising method for rapid volumetric heating, higher reaction rates, and shorter reaction times. As a result, this has opened up the possibility of realizing fast synthesis of nanomaterials in a very short time [26, 27]. Recently, we have successfully synthesized single-crystalline NiO nanosheets by a precursor convention method [28]. Herein,

Z.-H. Liang · Y.-J. Zhu (✉) · G.-F. Cheng · Y.-H. Huang
State Key Laboratory of High Performance Ceramics and Superfine Microstructure, Shanghai Institute of Ceramics, Chinese Academy of Sciences, Shanghai 200050, P. R. China
e-mail: y.j.zhu@mail.sic.ac.cn

we report the synthesis of ZnO nanosheets by room-temperature decomposition of a layered precursor, which was synthesized using zinc acetate and ethylene glycol by microwave heating. The strategy for synthesis of ZnO was illustrated in Fig. 1. The combination of microwave-heating and our synthetic strategy makes the preparation process convenient, simple and efficient. The preparation was carried out at relatively low temperatures without using any template, surfactant or seed, which avoided the subsequent complicated workup procedure for removal of the template or seed.

Experimental procedure

All chemicals were analytical grade and used as purchased without further purification. Zinc acetate and ethylene glycol (EG) were purchased from Shanghai Chemical Reagents Company. ZnO nanosheets were synthesized by two steps. The precursor was synthesized by the following step (step 1): 0.44 g of $Zn(CH_3COO)_2 \cdot 2H_2O$ was added into 20 ml EG in a 50-ml round-bottomed flask. The mixture was heated by microwave. The microwave oven (2.45 GHz) used was a focused single-mode microwave synthesis system (Discover, CEM, USA). The temperature was controlled by automatically adjusting microwave power. After the mixture was cooled to room temperature, the product was separated by centrifugation and washed with absolute ethanol twice and dried in a vacuum at 60°C. ZnO nanosheets were synthesized by the second step: the precursor synthesized by above method was added to 20 ml deionized water. The mixture was stirred for 24 h at room temperature or heated by microwave at 100°C for 10 min. The products were separated by centrifugation, washed with deionized water three times and dried in a vacuum. Experimental conditions for preparation of some typical ZnO nanosheet samples were given in Table 1.

X-ray diffraction (XRD) patterns were carried out on a Rigaku D/max 2550V X-ray diffractometer with CuK_α radiation and on a Huber G 670 diffractometer using graphite-monochromatized high-intensity $CuK_{\alpha 1}$ radiation. Transmission electron microscopy (TEM) images and electron diffraction (ED) patterns were obtained on JEOL JEM-2010 and JEOL JEM-2100F field-emission transmission electron microscopes. Differential scanning calorimetric analysis (DSC) and thermogravimetric analysis (TG) were carried out with a STA-409PC/4/H Luxx simultaneous TG-DTA/DSC apparatus (Germany) with a heating rate of 10°C min^{-1} in flowing air. UV–Vis absorption spectra were carried out on a UV-2300 spectrophotometer (Techcomp, China).

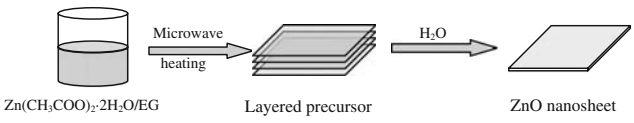

Fig. 1 Scheme of the strategy for synthesis of ZnO nanosheets

Results and discussion

Synthetic temperature of the layered precursor has important effect on the formation of the products. No solid products were obtained while the synthetic temperature was lower than 150°C. The product synthesized at 165°C or higher was typical of layer-structured compound. Figure 2a shows the XRD pattern of the precursor synthesized by microwave heating 0.1 M $Zn(CH_3COO)_2 \cdot 2H_2O$ in EG at 176°C for 5 min. The strong peak in XRD pattern of the precursor corresponds to an interlayer spacing of 10.9 Å, which is typical of the layer-structured compound. The thermal behavior of the layered precursor was investigated with TG and DSC measurements (Fig. 3). The TG curve showed that the weight loss began at 60°C. The major weight loss occurred rapidly between 320 and 390°C. The total weight loss was measured to be ~35%, which was close to the value (34.1%) calculated from the following reaction:

$$Zn_5(OH)_8(CH_3COO)_2 \cdot 2H_2O + O_2 \rightarrow 5ZnO + H_2O + CO_2 \quad (1)$$

The DSC curve showed an exothermic peak with a maximum located at 376°C, which fits well with that of weight loss in the TG curve, corresponding to exothermic behavior during the decomposition of zinc acetate hydroxide $Zn_5(OH)_8(CH_3COO)_2 \cdot 2H_2O$ to ZnO. The layered precursor prepared by our method may be $Zn_5(OH)_8(CH_3COO)_2 \cdot 2H_2O$.

It was interesting that the layered precursor was unstable in water and was able to decompose to ZnO. According to this property, aqueous solution route was used to synthesize ZnO nanosheets from the layered precursor. Figure 2b–d show XRD patterns of the products synthesized from the layered precursor at different conditions. No peaks due to the layered precursor were observed in XRD patterns and all peaks can be indexed to a single phase of crystalline ZnO with the hexagonal structure (JCPDS No.

Table 1 Experimental conditions for preparation of some typical ZnO nanosheet samples and their morphologies

Sample	Step 1		Step 2			Morphologies
	T (°C)	Time (min)	Solvent	T (°C)	Time	
1	<150	5				No products
2	165	5	H_2O	25	24 h	Nanosheets, particles
3	176	5	H_2O	25	24 h	Nanosheets
4	176	10	H_2O	25	24 h	Nanosheets
5	176	30	H_2O	25	24 h	Multi-layer nanosheets
6	176	10	0.05 M NaOH	25	24 h	Nanosheets
7	176	5	H_2O	100	10 min	Nanosheets

80-0075). These results show that the layered precursor can completely decompose and form crystalline ZnO in water or in NaOH aqueous solution.

The morphologies of ZnO samples were investigated by TEM, as shown in Fig. 4. TEM micrograph of sample 2 synthesized from the precursor prepared at 165 °C for 5 min was shown in Fig. 4a, one can see that nanosheets as well as nanoparticles were observed. Compared with sample 2, sample 3 synthesized under the same condition except that synthetic temperature of the precursor was increased to 176°C. Sample 3 (Fig. 4b) was mainly composed of ZnO nanosheets with lateral sizes up to 360 nm. In a few cases, curled ZnO nanosheets were observed (the top right corner of Fig. 4b). The thickness of ZnO nanosheets was about 5 nm estimated from standing and curled ZnO nanosheets. Figure 4c shows sample 4 synthesized from the precursor prepared at 176°C for 10 min. Compared with sample 3, the lateral sizes of ZnO nanosheets in sample 4 were larger and up to 1 μm. Figure 4d shows

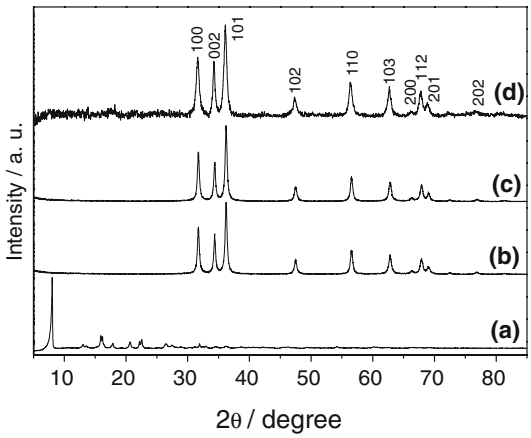

Fig. 2 XRD patterns of samples. (**a**) The layered precursor prepared by microwave heating 0.44 g $Zn(CH_3COO)_2 \cdot 2H_2O$ in 20 ml EG at 176°C for 5 min; (**b**) sample 3; (**c**) sample 4; (**d**) sample 7

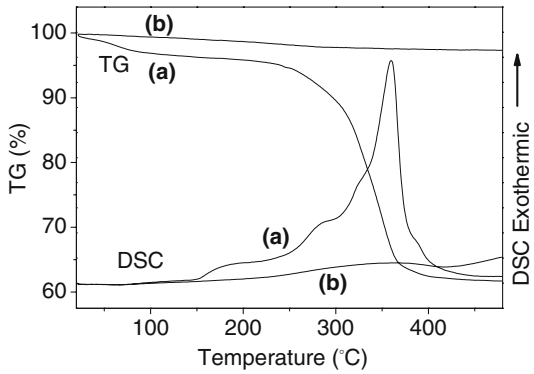

Fig. 3 Differential scanning calorimetric analysis (DSC) and thermogravimetric analysis (TG) curves (**a**) the layered precursor; (**b**) sample 3

several overlapped ZnO nanosheets and their ED pattern. The ED pattern can be indexed as the $[1\bar{2}10]$ zone axis of single-crystalline hexagonal wurtzite ZnO. High-resolution transmission electron microscopy (HRTEM) image (Fig. 4e) is consistent with the ED pattern in Fig. 4d, indicating ZnO nanosheets were single-crystalline with structural defects. Some ZnO nanosheets were curled (Fig. 4f), indicating ZnO nanosheets were very thin. The thicknesses of ZnO nanosheets was about 10 nm estimated from standing and curled nanosheets, which was larger than that of sample 3. Sample 5 (Fig. 4g), which was synthesized at the same condition as sample 3 except that the precursor was prepared at 176°C for 30 min, consisted mainly of multi-layered nanosheets with elliptical shape and with lateral sizes ranging from 200 to 500 nm. Figure 4h shows a typical ZnO nanosheet with elliptical shape. Figure 4i shows another single multi-layered nanosheet. The corresponding ED pattern and HRTEM image shown in Fig. 4j, k, respectively, were recorded with electron beam perpendicular to the nanosheet surface. The ED pattern can be indexed as the $[1\bar{2}10]$ zone axis of single-crystalline hexagonal

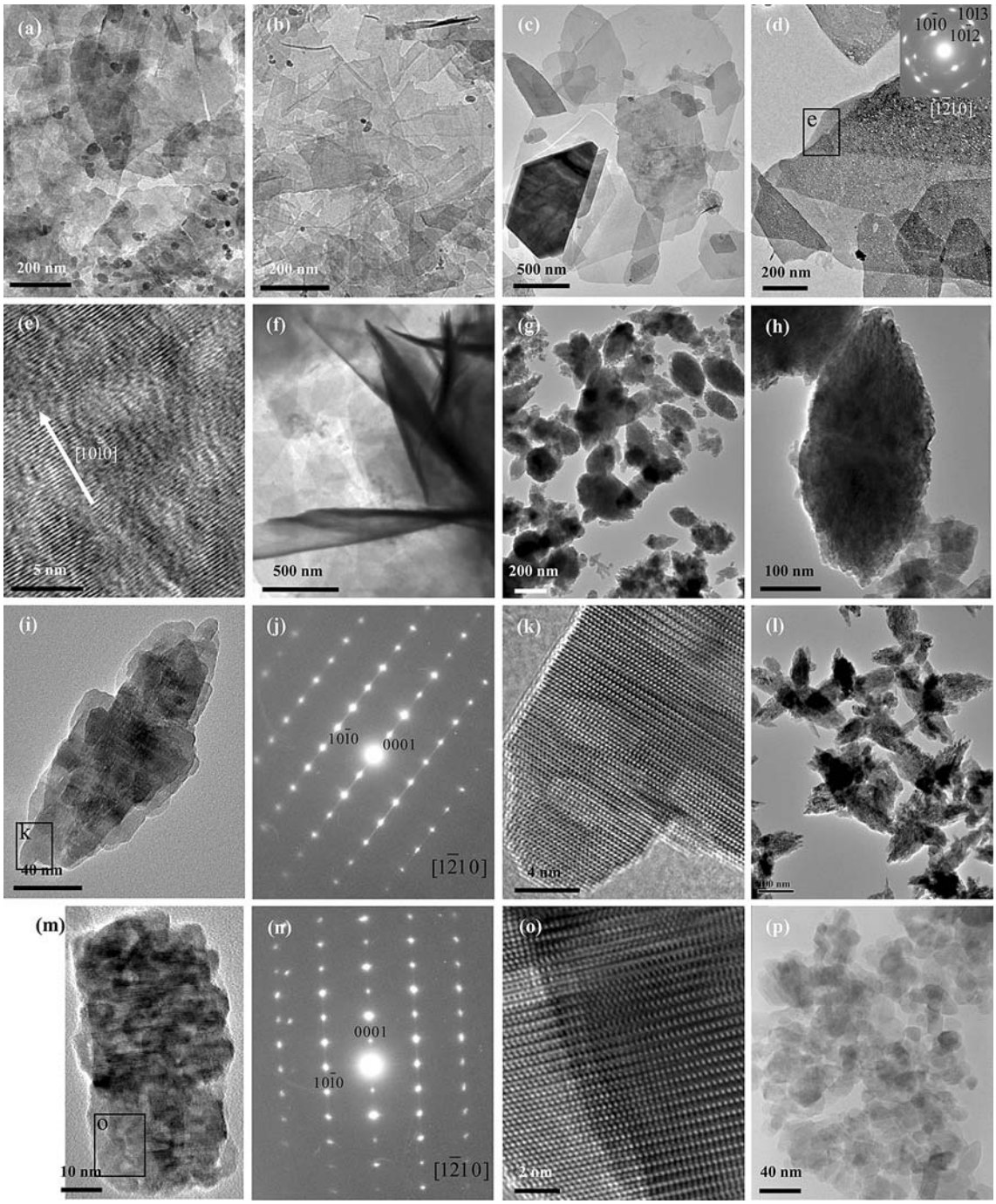

Fig. 4 TEM, HRTEM images and ED patterns of ZnO samples. (**a**) Sample 2; (**b**) sample 3; (**c**)–(**f**) sample 4; (**g**)–(**k**) sample 5; (**l**)–(**o**) sample 6; (**p**) sample 7

wurtzite ZnO, consistent with the XRD result. ED patterns taken from different nanosheets were essentially the same, suggesting the plane of ZnO nanosheets was $\pm(1\bar{2}10)$. HRTEM images taken from different nanosheets are essentially the same as Fig. 4k. The interplanar spacings were measured to be 5.2 and 2.8 Å, corresponding to (0001) and $(10\bar{1}0)$, respectively. These results further verified the $\pm(1\bar{2}10)$ orientation of ZnO nanosheets.

A further experiment using NaOH aqueous solution to investigate the effect of an alkaline environment on the ZnO morphology, it was found that ZnO immediately formed in aqueous NaOH solution at room temperature. The lateral sizes of ZnO nanosheets were

in the range of 50–200 nm (Fig. 4l). Figure 4n, o show an ED pattern and a HRTEM image of a single ZnO nanosheet in Fig. 4m. The ED pattern and HRTEM image indicates that the ZnO nanosheets were single-crystalline in structure.

Sample 7, prepared by microwave-heating the layered precursor in deionized water at 100°C for 10 min, was composed of small ZnO crystallites with sizes ranging from 10 to 50 nm (Fig. 4p). ZnO crystallites had sheet shape and they overlapped each other.

Base on the experimental results, we propose the formation mechanism of ZnO nanosheets as follows:

In step 1, the layered precursor $Zn_5(OH)_8(CH_3COO)_2 \cdot 2H_2O$ was formed by microwave-heating a EG solution of $Zn(CH_3COO)_2 \cdot 2H_2O$. The reaction equation is as follows:

$$5Zn(CH_3COO)_2 \cdot 2H_2O = Zn_5(OH)_8(CH_3COO)_2 \cdot 2H_2O + 8CH_3COOH \quad (2)$$

In step 2, the layered precursor $Zn_5(OH)_8(CH_3COO)_2 \cdot 2H_2O$ was decomposed in water to form ZnO nanosheets. The reaction equations involved in the formation of ZnO nanosheets are shown below:

$$H_2O = H^+ + OH^- \quad (3)$$

$$Zn_5(OH)_8(CH_3COO)_2 \cdot 2H_2O + 2OH^- = 5Zn(OH)_2 + 2H_2O + 2CH_3COO^- \quad (4)$$

$$2Zn(OH)_2 = 2ZnO + 2H_2O \quad (5)$$

$$CH_3COO^- + H^+ = CH_3COOH \quad (6)$$

The nanosheets could be easily prepared for those compounds with a layered structure. For the compound without a layered structure, a layered precursor conversion method has been successfully demonstrated for the preparation of nanosheets [28, 29]. ZnO has a hexagonal structure instead of a layered structure. The layered precursor conversion strategy is used for the preparation of ZnO nanosheets here, as shown in Fig. 1. In aqueous solution, CH_3COO^- in the precursor was replaced by OH^-, resulting in the formation of $Zn(OH)_2$, which decomposed to form ZnO nanosheets. The reaction rate was greatly affected by OH^- and temperature. In deioned water at room temperature, the reaction was slow due to low concentration of OH^-. The pH value of the solution after reaction was measured to be about 5, which is consistent with the aforementioned reaction equations. In NaOH aqueous solution, the reaction was rapid due to high concentration of OH^-, resulting in rapid formation of ZnO nanosheets. At an elevated temperature, the layered precursor rapidly decomposed and break up due to the increased reaction rate, resulting in the rapid formation of small ZnO nanosheets.

The thermal properties of ZnO nanosheet samples were investigated by TG/DSC measurements. TG curve of sample 3 (Fig. 3b) shows that the total weight loss is less than 3% up to 480°C. The corresponding DSC curve has no obvious exothermic or endothermic peak in the temperature range measured. TG/DSC curves of other samples are similar to sample 3. These results further demonstrates the layered precursor have decomposed completely to form ZnO. The weight loss may be due to the water adsorbed on the surface of ZnO nanosheets.

Fig. 5 shows the UV–Vis absorption spectra of ZnO nanosheets dispersed in absolute alcohol. Figure 5a shows the UV–Vis absorption spectrum of the precursor whose absorption edge was close to 200 nm. Figure 5b–f shows the absorption spectra of samples 3–7, respectively. One can see that the absorption spectra of these ZnO nanosheet samples are similar, with centers of absorption peaks around 358 nm (3.46 eV).

Conclusions

In summary, powders of ZnO nanosheets with the hexagonal structure have been successfully synthesized

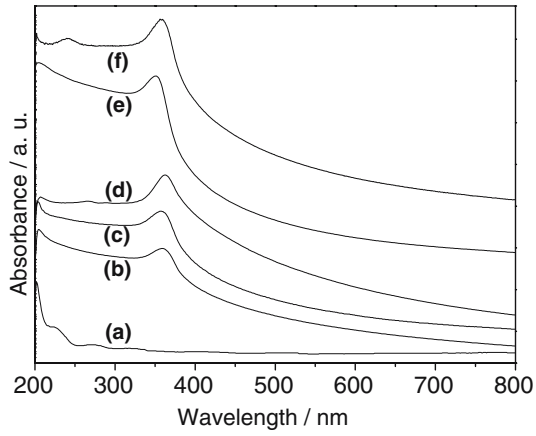

Fig. 5 UV–Vis absorption spectra of samples dispersed in absolute ethanol. (**a**) The precursor; (**b**) sample 3; (**c**) sample 4; (**d**) sample 5; (**e**) sample 6; (**f**) sample 7

by room-temperature decomposition of a layered precursor which was synthesized using zinc acetate and ethylene glycol by microwave heating. The thicknesses of ZnO nanosheets are in the range of 5–10 nm and lateral sizes up to 1 μm. The surfaces of ZnO nanosheets were parallel to the $\pm(1\bar{2}10)$ planes of the wurtzite structure. This method is fast, simple, low-temperature and low-cost for synthesis of ZnO nanosheets. The method can be easily scaled up for large scale production. We expect that this method can also be extended to synthesize nanosheets of other kinds of metal oxides.

Acknowledgements Financial support from National Natural Science Foundation of China (50472014) and Chinese Academy of Sciences under the Program for Recruiting Outstanding Overseas Chinese (Hundred Talents Program) is gratefully acknowledged. We thank the Fund for Innovation Research from Shanghai Institute of Ceramics, Chinese Academy of Sciences and the Natural Science Foundation from Science and Technology Committee of Shanghai (03ZR14104), P. R. China.

References

1. Xia YN, Yang PD, Sun YG, Wu YY, Mayers B, Gates B, Yin YD, Kim F, Yan HQ (2003) Adv Mater 15:353
2. Sasaki T, Ebina Y, Kitami Y, Watanabe M (2001) J Phys Chem B 105:6116
3. Sasaki T, Watanabe M (1997) J Phys Chem B 101:10159
4. Hu JQ, Bando Y, Zhan JH, Li YB, Sekiguchi T (2003) Appl Phys Lett 83:4414
5. Wang LZ, Omomo Y, Sakai N, Fukuda K, Nakai I, Ebina Y, Takada K, Watanabe M, Sasaki T (2003) Chem Mater 15:2873
6. Han YS, Park I, Choy JH (2001) J Mater Chem 11:1277
7. Miyamoto N, Nakato T (2002) Adv Mater 14:1267
8. Dai ZR, Pan ZW, Wang ZL (2002) J Phys Chem B 106:902
9. Sberveglieri G, Groppelli S, Nelli P, Tintinelli A, Giunta G (1995) Sens Actuators B 25:588
10. Rodriguez JA, Jirsak T, Dvorak J, Sambasivan S, Fischer D (2000) J Phys Chem B 104:319
11. Sang BS, Yamada A, Konagai M (1998) Jpn J Appl Phys 37:L206
12. Minami T (2000) MRS Bull 25:38
13. Lee CJ, Lee TJ, Lyu SC, Zhang Y, Ruh H, Lee HJ (2002) Appl Phys Lett 81:3648
14. Lee JJ, Kim YB, Yoon YS (2005) Appl Surf Science 244:365
15. Huang MH, Mao S, Feick H, Yan HQ, Wu YY, Kind H, Weber E, Russo R, Yang PD (2001) Science 292:1897
16. Goldberger J, Sirbuly DJ, Law M, Yang PD (2005) J Phys Chem B 109:9
17. Sun XH, Lam S, Sham TK, Heigl F, Jürgensen A, Wong NB (2005) J Phys Chem B 109:3120
18. Greene LE, Law M, Goldberger J, Kim F, Johnson JC, Zhang YF, Saykally RJ, Yang PD (2003) Angew Chem, Int Ed 42:3031
19. Pan ZW, Dai ZR, Wang ZL (2001) Science 291:1947
20. Chen SJ, Liu YC, Shao CL, Mu R, Lu YM, Zhang JY, Shen DZ, Fan XW (2005) Adv Mater 17:586
21. Fan HJ, Scholz R, Kolb FM, Zacharias M, Gösele U, Heyroth F, Eisenschmidt C, Hempel T, Christen J (2004) Appl Phys A 79:1895
22. Park JH, Park JG (2005) Appl Phys A 80:43
23. Hu PA, Liu YQ, Fu L, Wang XB, Zhu DB (2005) Appl Phys A 80:35
24. Gedye R, Smith F, Westaway K, Humera A, Baldisera L, Laberge L, Rousell L (1986) Tetrahedron Lett 27:279
25. Giguere R, Bray TL, Duncan SM, Majetich G (1986) Tetrahedron Lett 27:4945
26. Zhu YJ, Wang WW, Qi RJ, Hu XL (2004) Angew Chem Int Ed 43:1410
27. Liang ZH, Zhu YJ (2004) Chem Lett 33:1314
28. Liang ZH, Zhu YJ, Hu XL (2004) J Phys Chem B 104:3488
29. Liang ZH, Zhu YJ (2005) Chem Lett 34:214